Supporting Information

Surface-halogen-introduced 2D NiCo bimetallic MOFs via modulation method for elevated electrochemical glucose sensing

Panpan Li[a], Yang Bai*[b,c], Guangxun Zhang[a], Xiaotian Guo[a], Xiangren Meng[d], Huan Pang*[a]

a School of Chemistry and Chemical Engineering, Yangzhou University, Yangzhou, Jiangsu, 225009, China

b School of Pharmacy, Changzhou University, Changzhou, Jiangsu, 213164, P. R. China

c State Key Laboratory of Coordination Chemistry, Nanjing University, Nanjing, Jiangsu, 210023, P. R. China

d School of Tourism and Cuisine, Yangzhou University, Yangzhou 225127, China

*Corresponding authors: huanpangchem@hotmail.com; panghuan@yzu.edu.cn

Experimental Section

Preparation of cuboid MOFs

4,4'-bipyridine (2 mmol, 0.31 g), $NiSO_4·6H_2O$ (0.5 mmol, 0.13 g) and $CoSO_4·7H_2O$ (1.5 mmol, 0.42 g) were added into a 50 mL Teflon-lined stainless autoclave. Water (15 mL) was then added and stirred under room temperature for 10 min. Then 7.5 mL EtOH was added into the clave and heated at 100 °C for 24 h. After cooling down to the room temperature, solid product was collected by centrifugation. The solid was then washed with ethanol (10 mL *3) and water (10 mL *3) dried at 50 °C under vacuum.

Preparation of 2D MOFs nanoplates

4,4'-bipyridine (2 mmol, 0.31 g), $NiSO_4·6H_2O$ (0.5 mmol, 0.13 g) and $CoSO_4·7H_2O$ (1.5 mmol, 0.42 g) were dissolved in 15 mL water and stirred at room temperature for 10 min, 4-bromopyridine (2.3 mmol, 0.5 g) or 4-iodopyridine (1.6 mmol, 0.5 g) was dissolved in 7.5 mL EtOH containing pyridine (12.4 mmol, 1.0 g), Then the solution was slowly added into the former solution under stirring, The clave was then sealed and heated at 100°C for 24 h. After cooling down to the room temperature, solid product was collected by centrifugation. The solid was then washed with ethanol (10 mL *3) and water (10 mL *3) dried at 50 °C under vacuum.

Characterization

The morphological features were characterized by field emission scanning electron microscopy (FESEM, Zeiss-Supra55), high resolution transmission electron microscopy (HRTEM, Tecnai G2 F30 S-TWIN), and energy dispersive X-ray spectrometry (EDS) mapping. X-ray diffraction (XRD) patterns were examined on a Bruker D8 Advanced X-

ray Diffractometer (Cu-Kα radiation: λ = 0.15406 nm). The chemical states were measured using an Axis Ultra X-ray photoelectron spectroscope (XPS, Kratos Analytical Ltd., UK) equipped with a standard monochromatic Al-Kα source (hv = 1486.6 eV). Fourier transform infrared (FTIR) transmission spectra were obtained on a BRUKER-EQUINOX-55 IR spectrophotometer. N_2 adsorption-desorption measurements were performed on Quantachrome Instruments, Autosorb IQ3.

Fabrication of working electrodes and electrochemical measurements

To fabricate the working electrodes, a mixture containing of the as-synthesized MOFs (3 mg), 5 wt% Nafion solution 25 μL, and 300 μL of water, 250 μL of ethanol was well mixed. Then the solution was ultrasonicated for one hour. 5 μL mixture was dripped on the surface of glassy carbon electrode and dried for two hours at room temperature.

Electrochemical measurements were conducted on a CHI660e electrochemical station (CH Instruments, Shanghai, China). A conventional three-electrode system was used for all electrochemical measurements, which consisted of a modified GCE electrode as the working electrode, an Ag/AgCl (saturated KCl) electrode as the reference electrode, and platinum foil as the auxiliary electrode in 0.1 M NaOH with the protection of N_2.
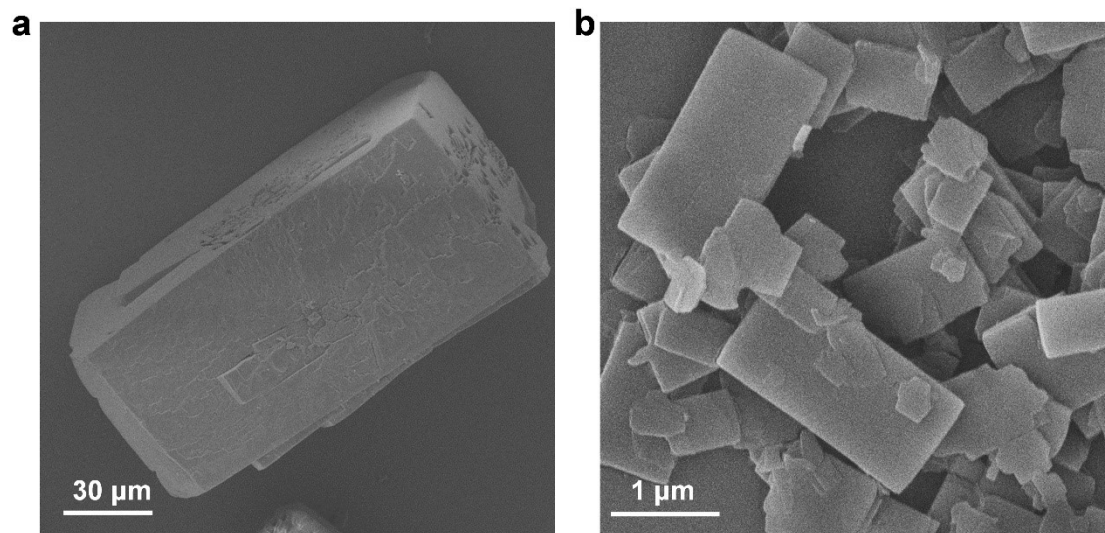
Figure S1 SEM images of (a) NiCoB, (b) NiCoBP.
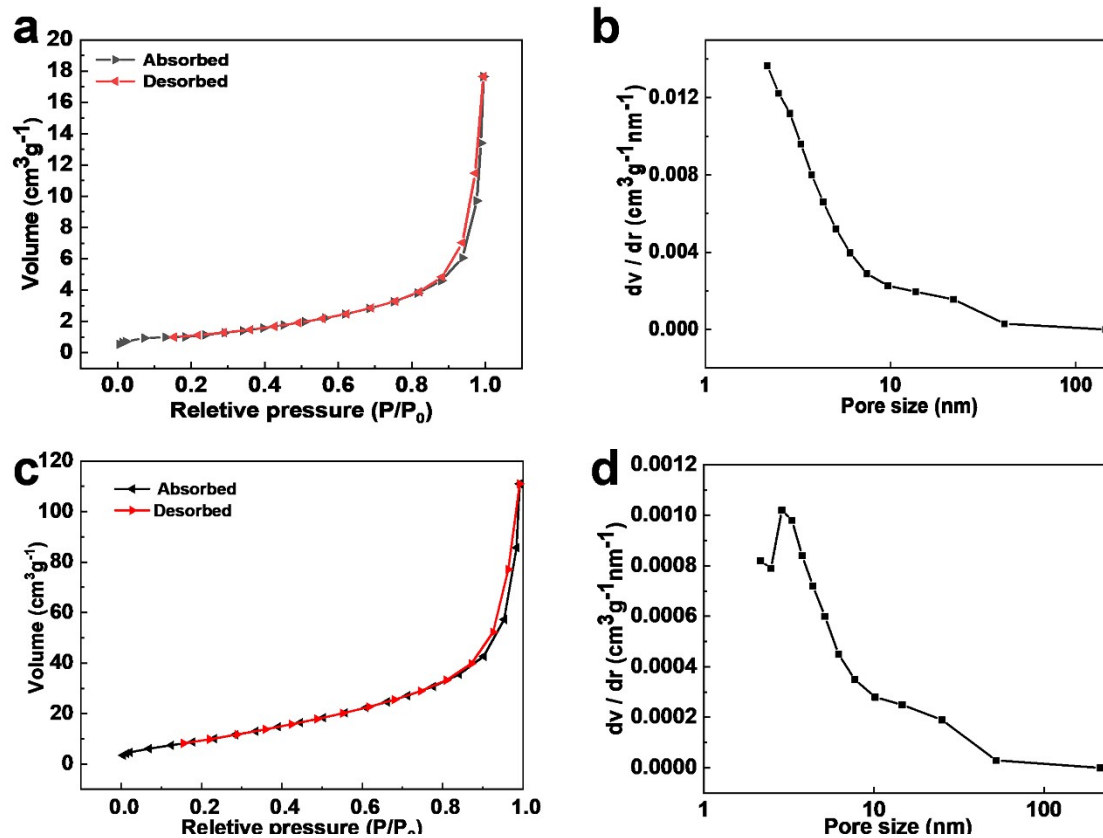
Figure S2 (a, b) Nitrogen adsorption-desorption isotherms of NiCoB and the corresponding pore size distribution at 77 K. (c, d) Nitrogen adsorption-desorption isotherms of NiCoBP and the corresponding pore size distribution at 77 K.
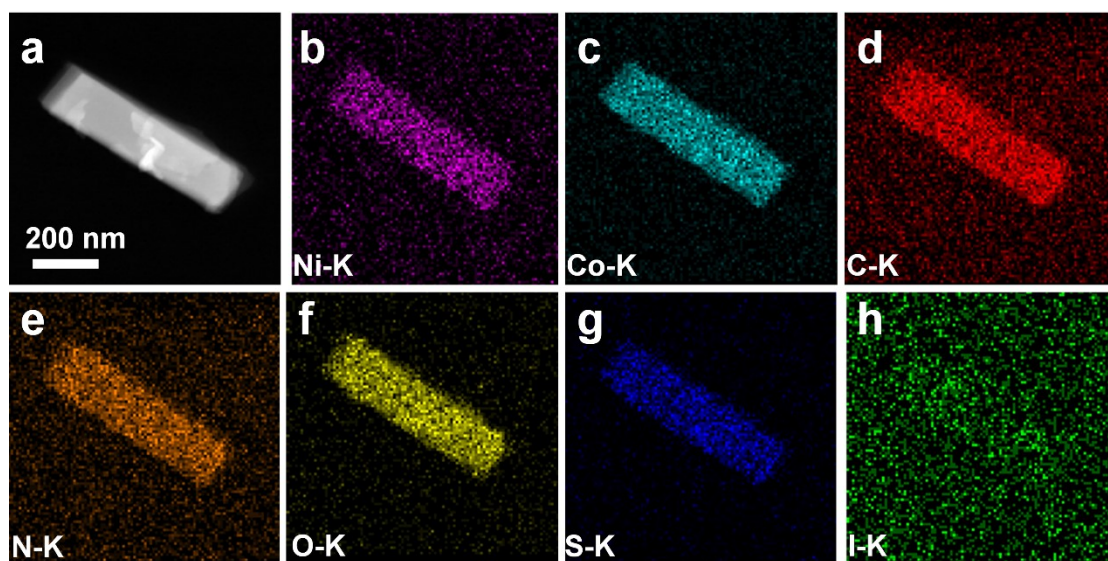
Figure S3 HAADF-STEM and elemental mappings of Ni-K, Co-k, C-K, N-K, O-K, S-K, and I-k in NiCoBP-I.

a
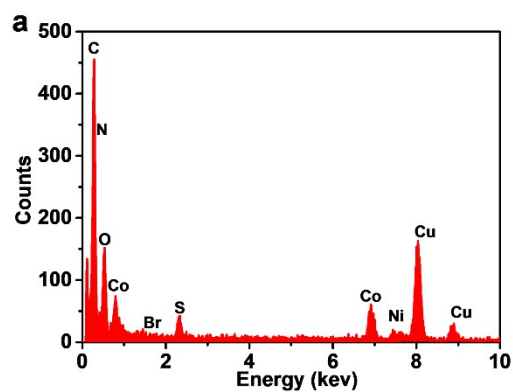
b

Element	Atomic content / %
C (K)	65.38
N (K)	8.47
O (K)	17.87
S (K)	2.24
Co (K)	4.64
Ni (K)	1.24
Br (L)	0.13

c
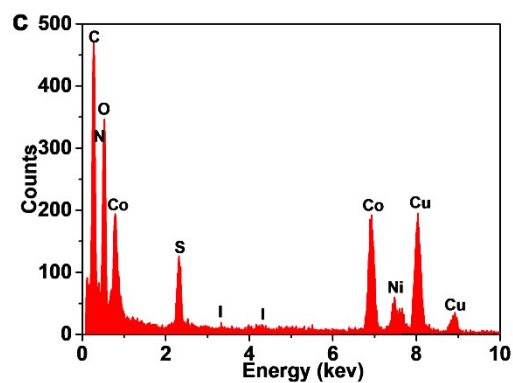
d

Element	Atomic content / %
C (K)	83.43
N (K)	4.01
O (K)	9.89
S (K)	0.77
Co (K)	1.45
Ni (K)	0.83
I (L)	0.04

Figure S4 EDX spectrum and atomic content of each element of (a, b) NiCoBP-Br. (c, d) NiCoBP-I.
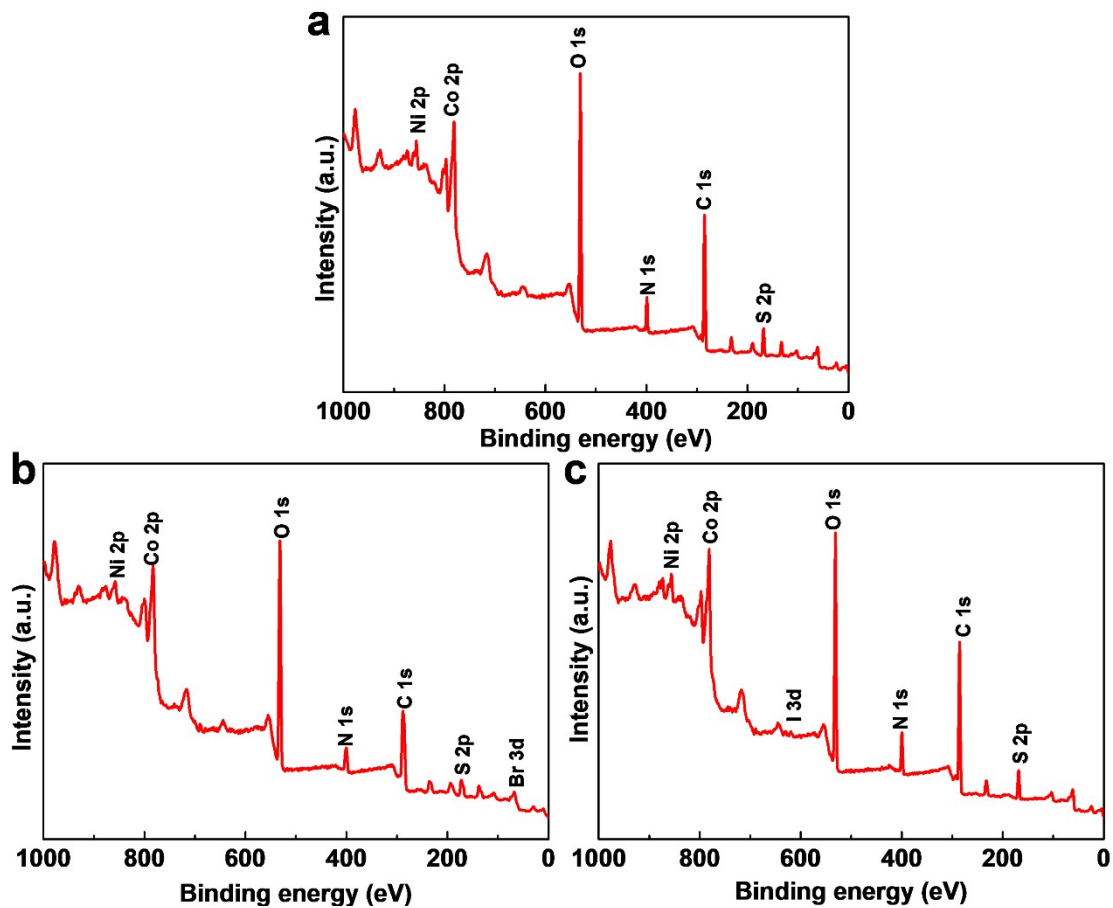
Figure S5 XPS survey spectra of (a) NiCoBP (b) NiCoBP-Br, (c) NiCoBP -I.
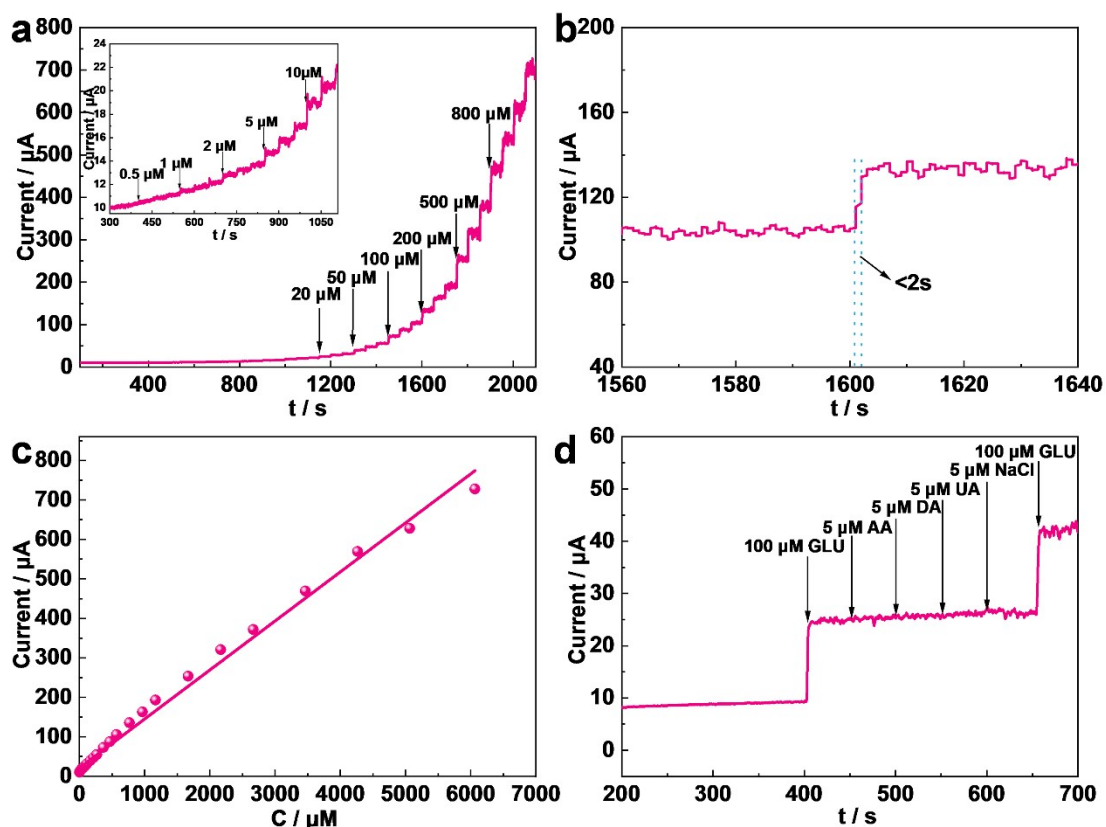
Figure S6 Electrochemical performances of the NiCoBP-Br GCE. (a) Current–time response of the NiCoBP-Br GCE at 0.55 V on successive additions of different amounts of GLU in 0.1 M NaOH. (b) Response time for NiCoBP-Br GCE after the addition glucose solution (c) A plot of electrocatalytic current of GLU versus its concentrations in the range of 0.5 μM to 6.065 mM. (d) Current–time response of the NiCoBP-Br GCE with the addition of 100 μM GLU, 5 μM AA, 5 μM DA, 5 μM UA, 5 μM NaCl, and 100 μM GLU into 0.1 M NaOH at 0.55 V.
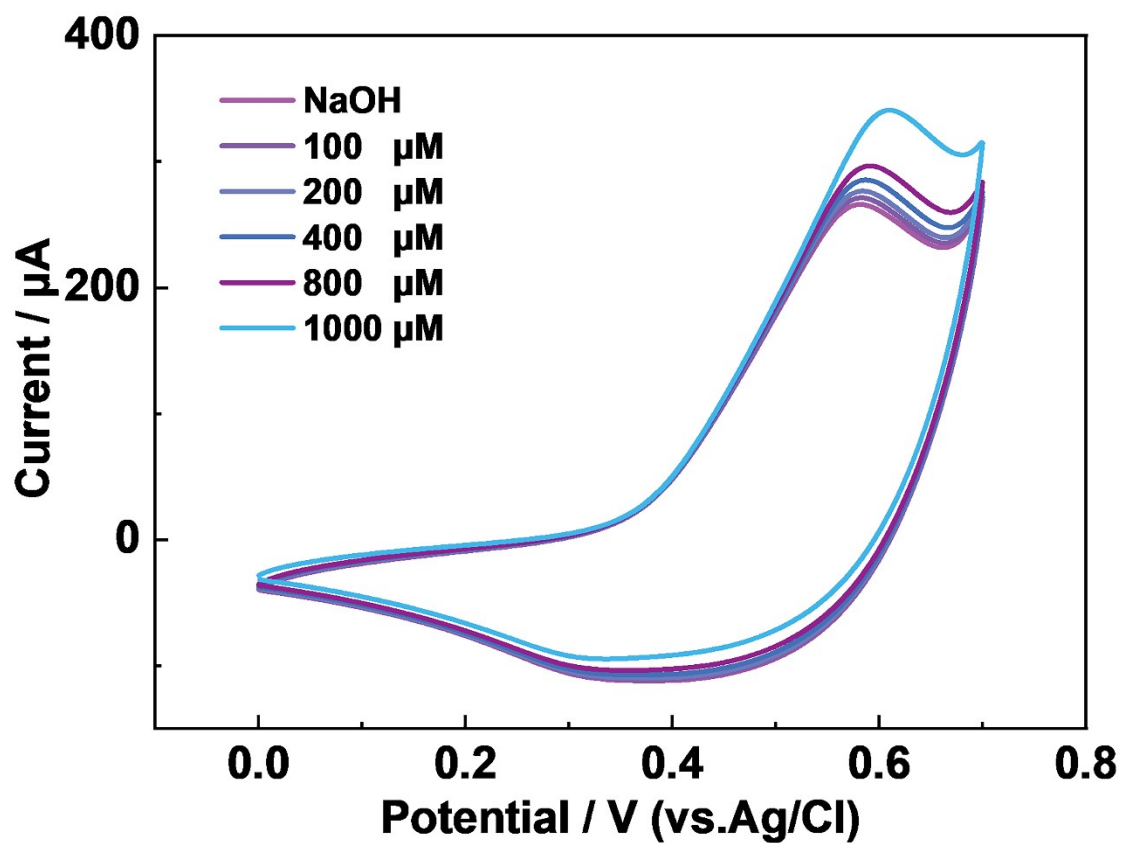
Figure S7 CV curves of NiCoBP GCE in NaOH (0.1 M) when adding different concentrations of GLU.
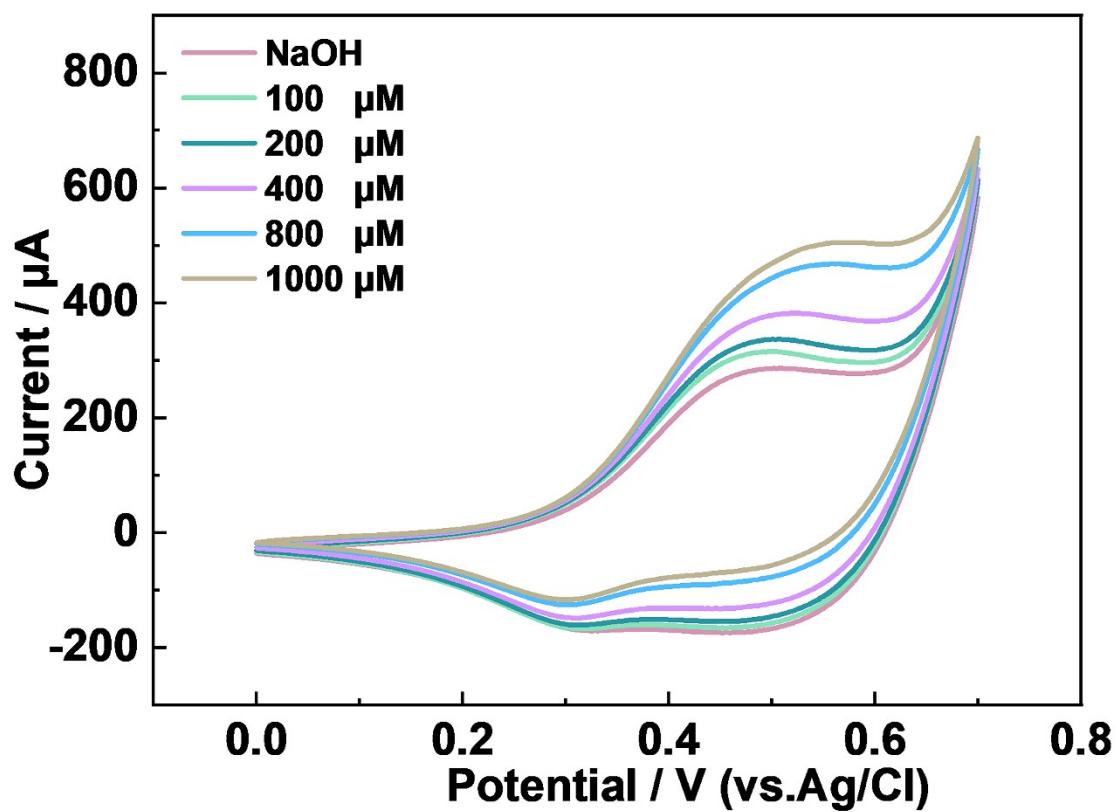
Figure S8 CV curves of NiCoBP-I GCE in NaOH (0.1 M) when adding different concentrations of GLU.
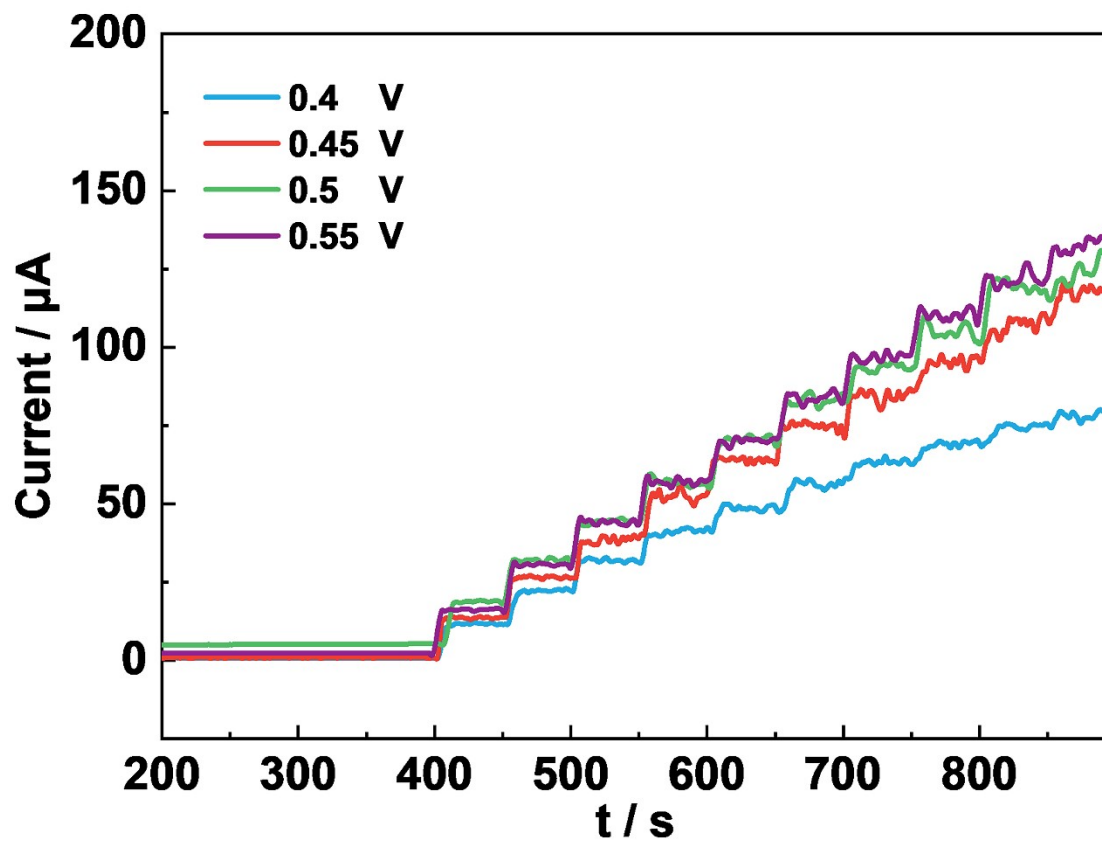
Figure S9 Amperometric responses of the NiCoBP GCE at different potentials (from 0.40 to 0.55 V) with continuous addition of 100 µM glucose in 0.1 M NaOH.
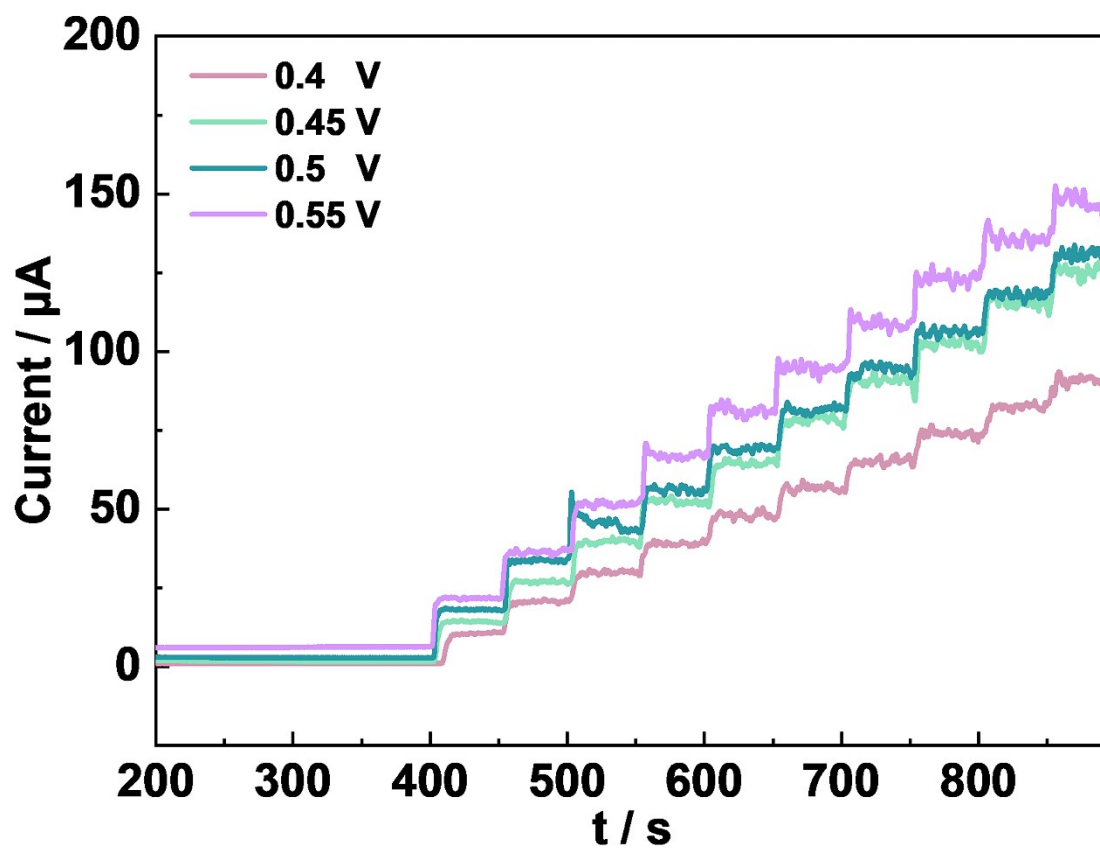
Figure S10 Amperometric responses of the NiCoBP-I GCE at different potentials (from 0.40 to 0.55 V) with continuous addition of 100 µM glucose in 0.1 M NaOH.
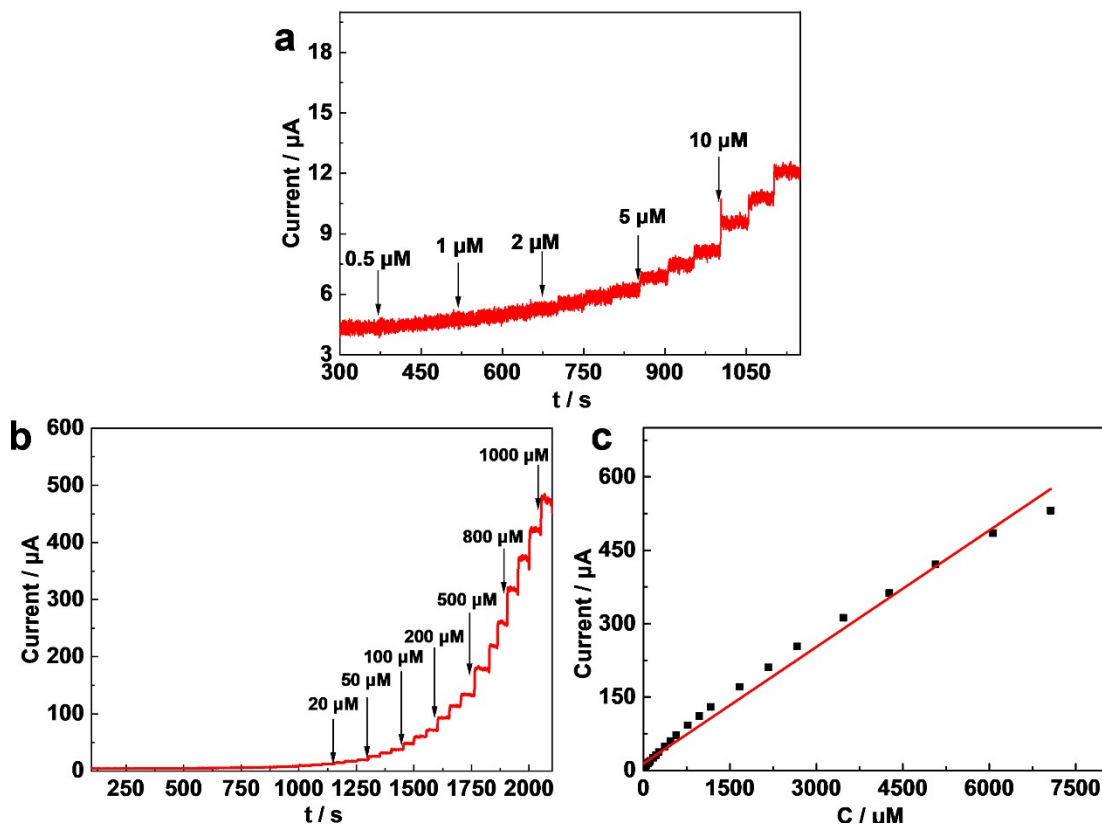
Figure S11 (a, b) Current–time response of the NiCoBP GCE at 0.55 V on successive additions of different amounts of GLU in 0.1 M NaOH. (c) A plot of electrocatalytic current of GLU versus its concentrations in the range of 0.5 µM to 7.065 mM.

The NiCoBP GCE exhibited a linear relationship between current responses and GLU concentration from 0.5 to 7065.5 µM, whose linear regression equation was I (µA) =14.34685 + 0.0794C (µM), R^2 = 0.9950, the sensitivity was about 1123.28 µA mM^{-1} cm^{-2}. The detection limit was as low as 0.104 µM with the S/N ratio of 3.
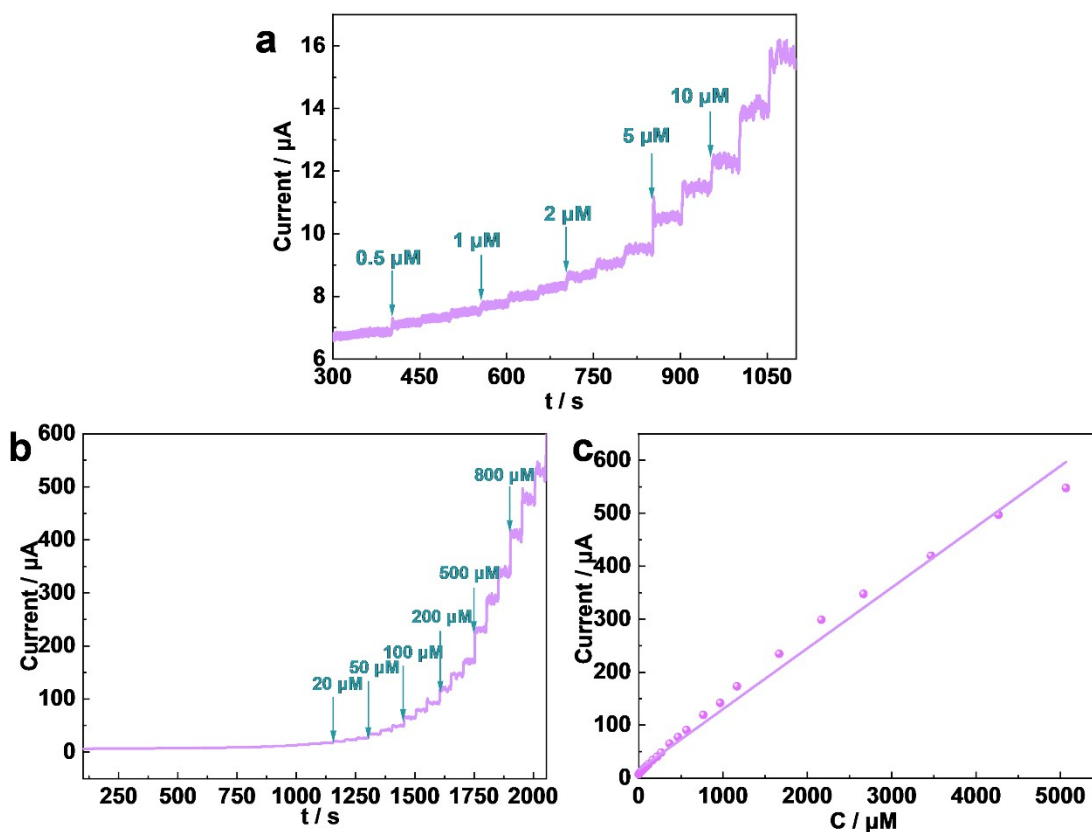
Figure S12 (a, b) Current–time response of the NiCoBP-I GCE at 0.55 V on successive additions of different amounts of GLU in 0.1 M NaOH. (c) A plot of electrocatalytic current of GLU versus its concentrations in the range of 0.5 µM to 6.065 mM.

The NiCoBP-I GCE exhibited a linear relationship between current responses and GLU concentration from 0.5 to 5065.5 µM, whose linear regression equation was I (µA) =15.8752 + 0.11465C (µM), R^2 = 0.9950, the sensitivity was about 1621.97 µA mM^{-1} cm^{-2}. The detection limit was as low as 0.072 µM with the S/N ratio of 3.
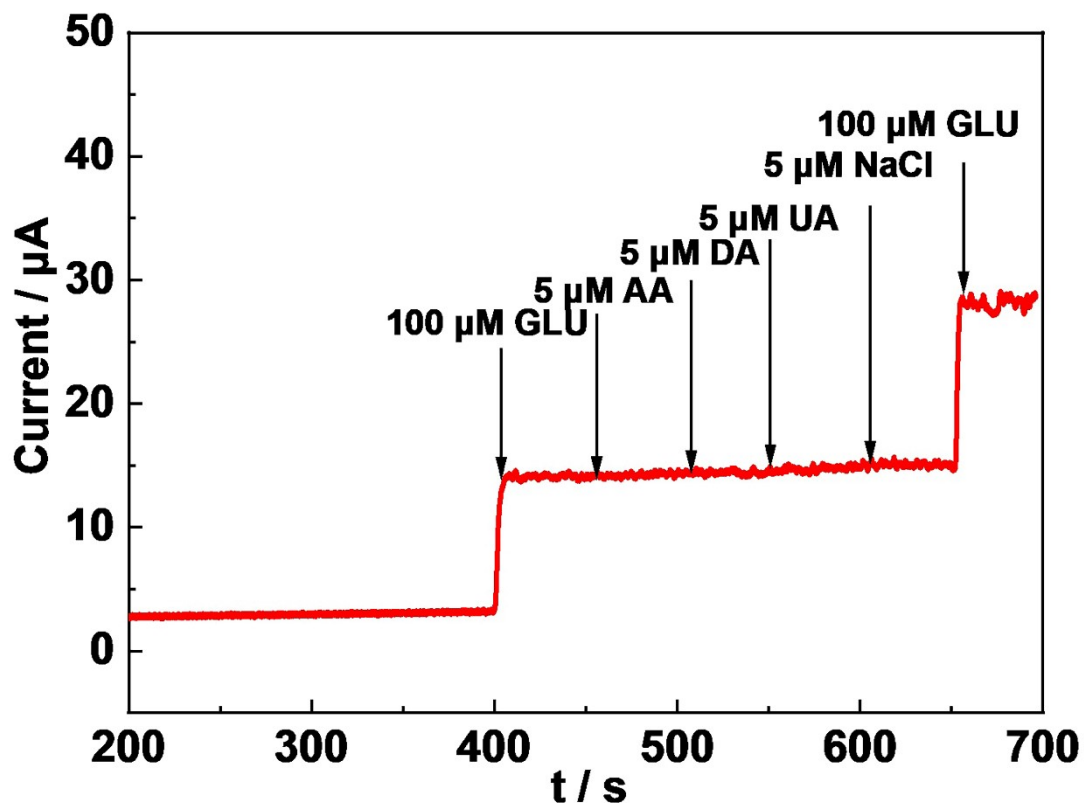
Figure S13 Current–time response of the NiCoBP GCE with the addition of 100 μM GLU, 5 μM AA, 5 μM DA, 5 μM UA, 5 μM NaCl, and 100 μM GLU into 0.1 M NaOH at 0.55 V.
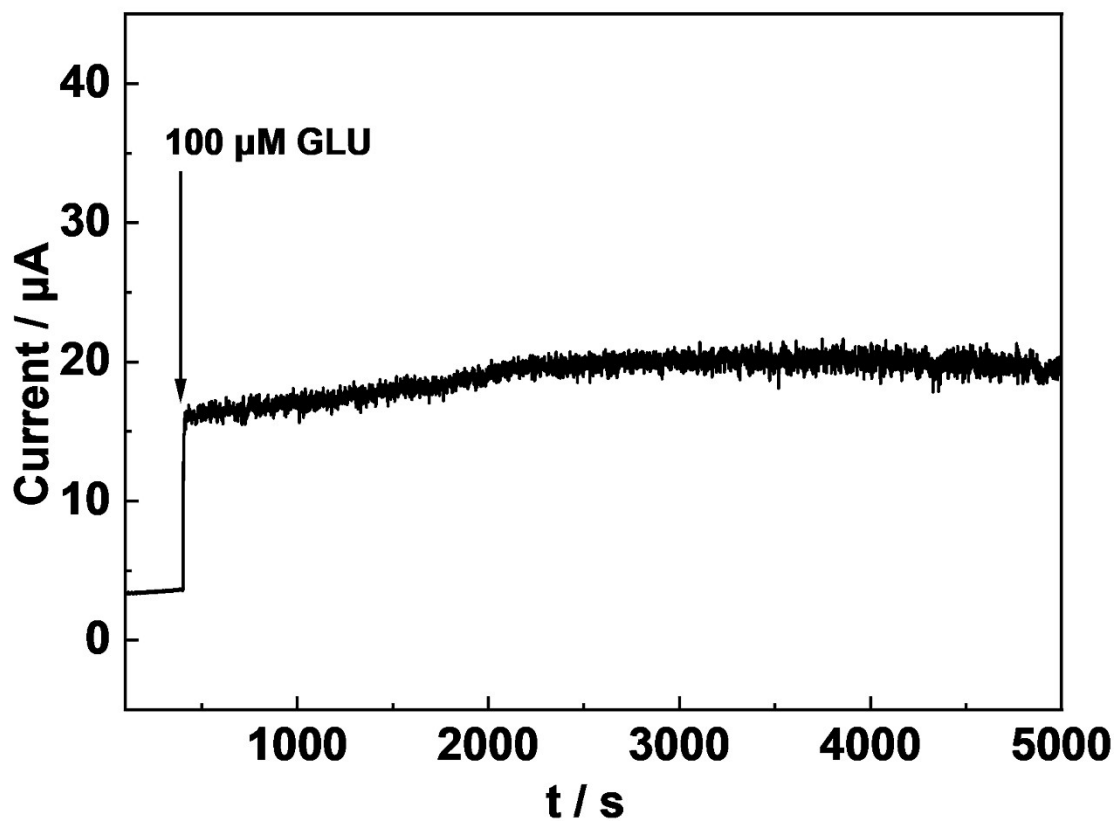
Figure S14 The stability of the response current for the NiCoBP GCE after the addition of GLU solution (100 μM) over 5000s.
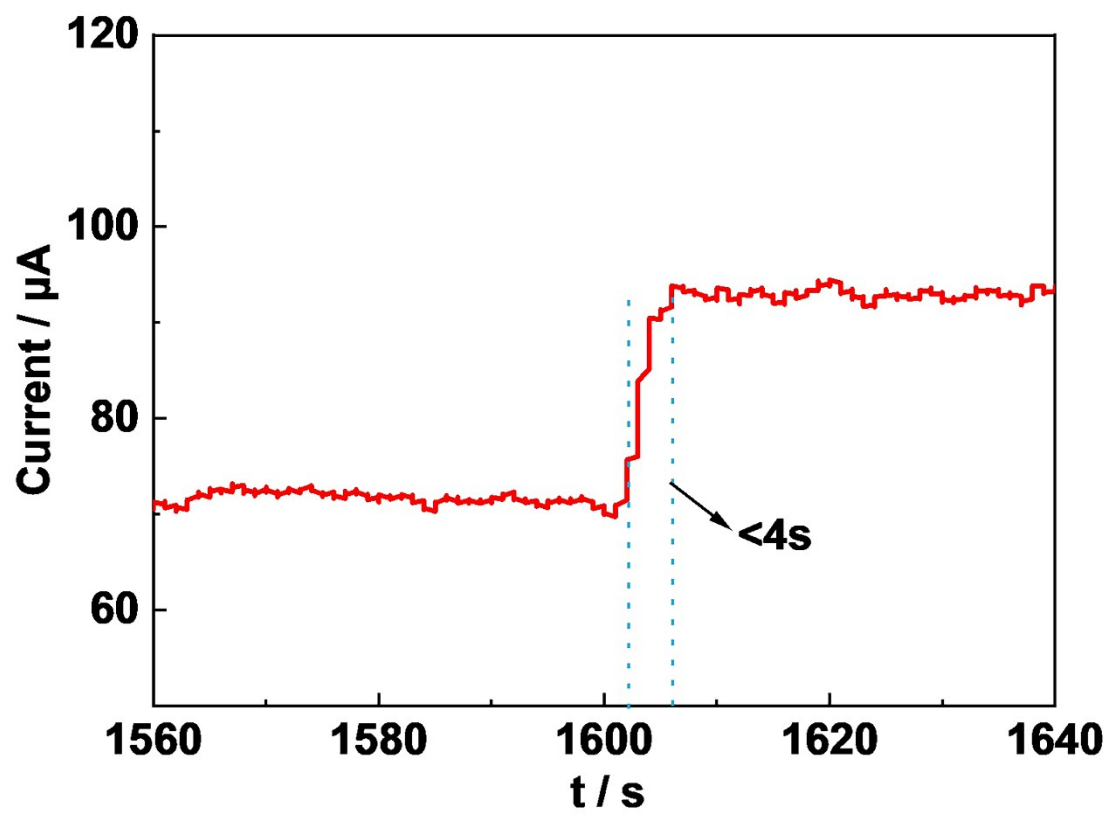
Figure S15 Response time for NiCoBP GCE after the addition glucose solution.
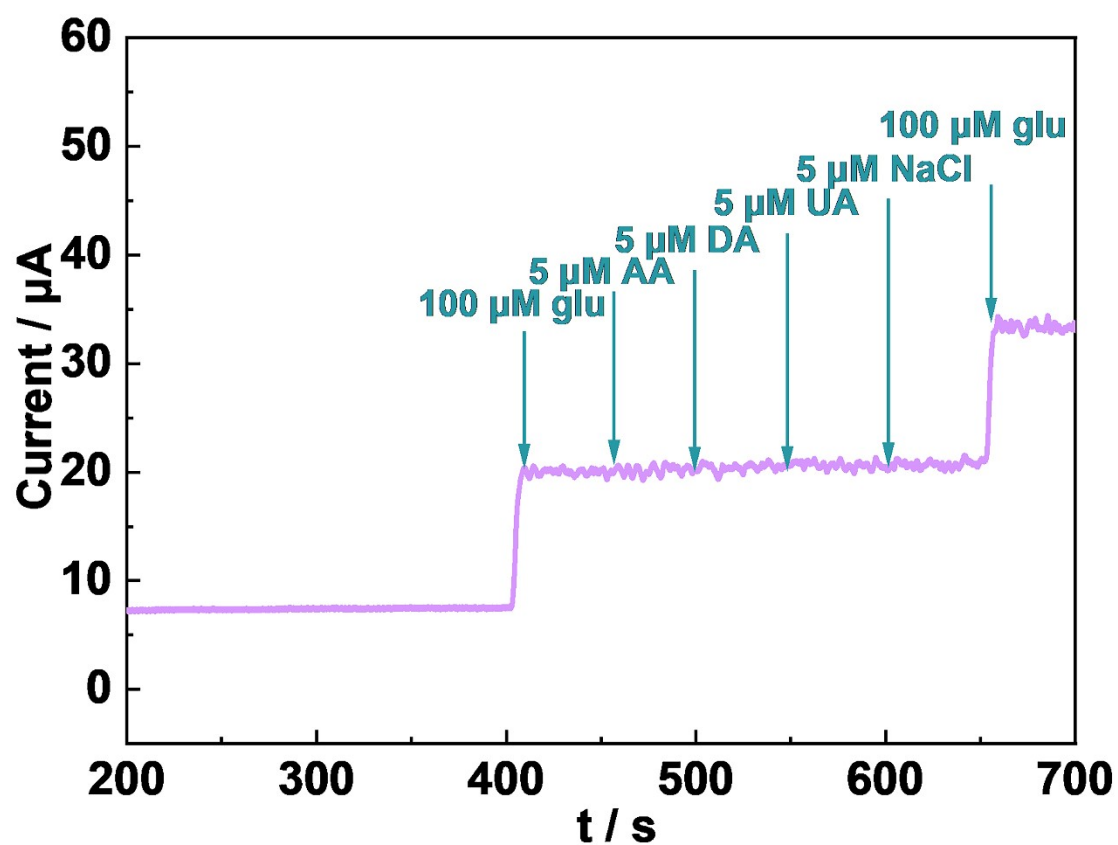
Figure S16 Current–time response of the NiCoBP-I GCE with the addition of 100 µM GLU, 5 µM AA, 5 µM DA, 5 µM UA, 5 µM NaCl, and 100 µM GLU into 0.1 M NaOH at 0.55 V.
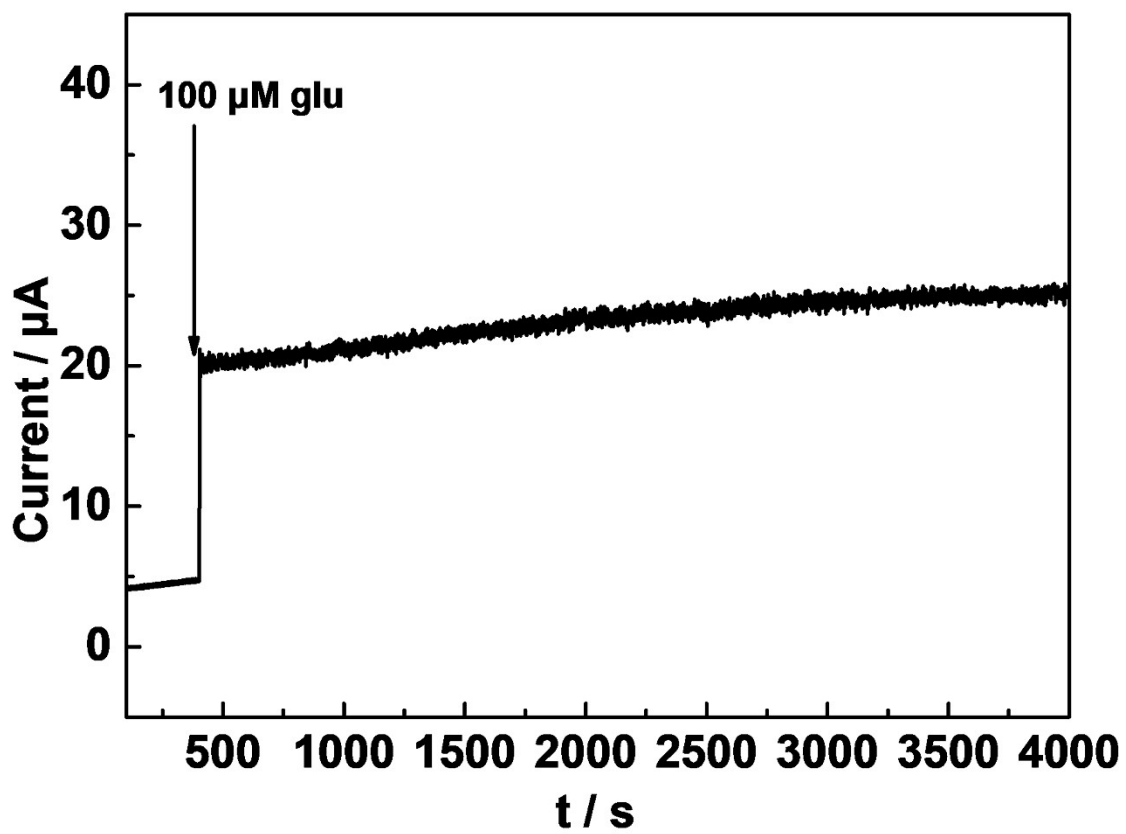
Figure S17 The stability of the response current for the NiCoBP-I GCE after the addition of GLU solution (100 μM) over 4000s.
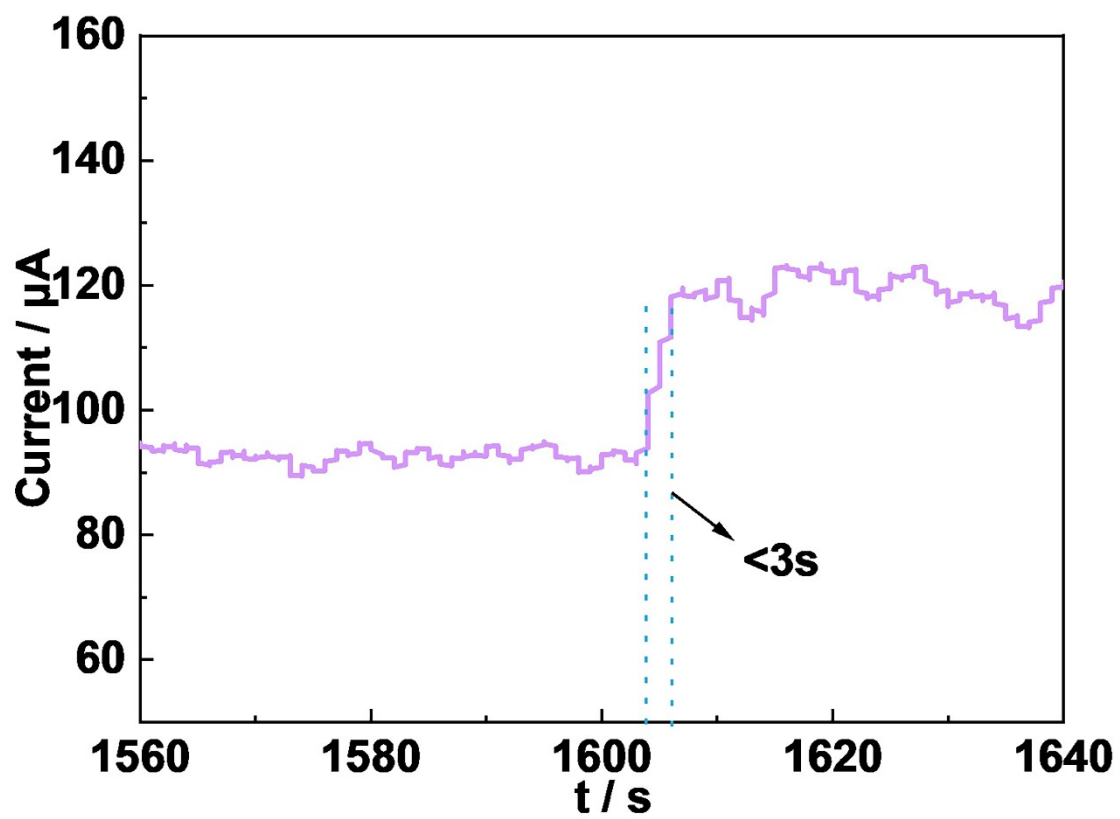
Figure S18 Response time for NiCoBP-I GCE after the addition glucose solution.
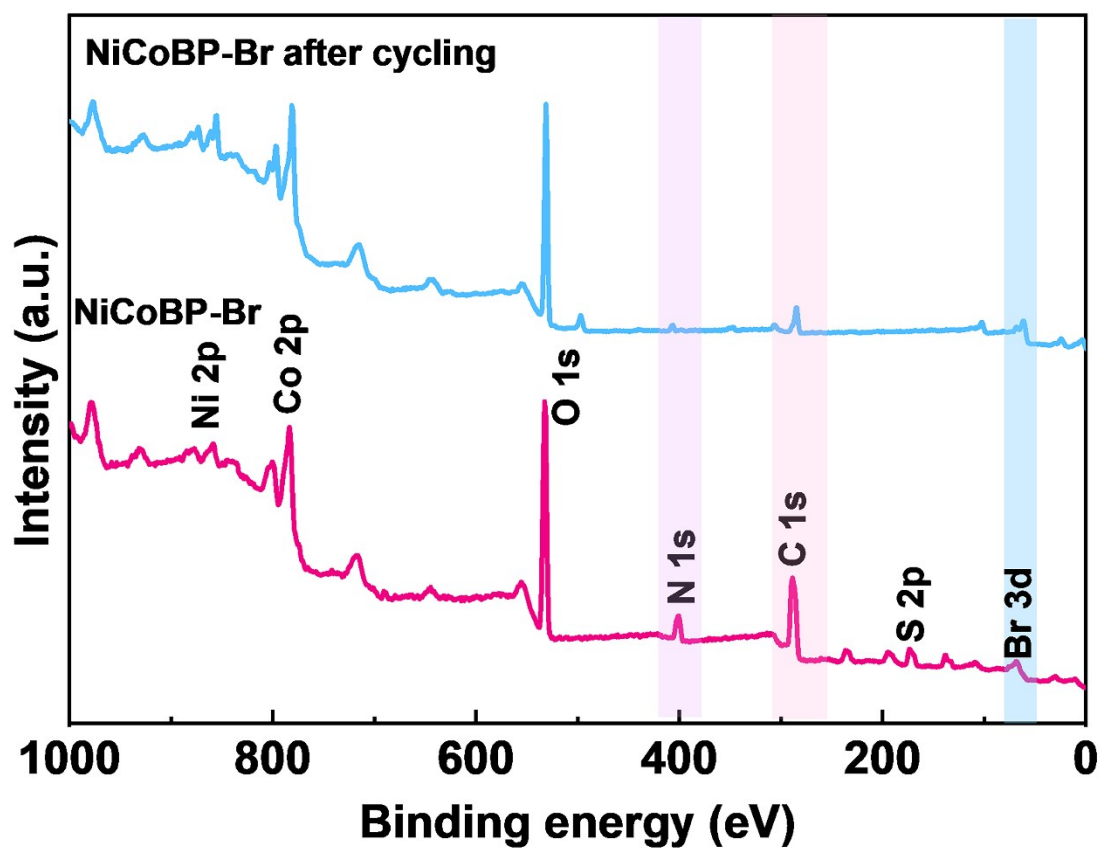
Figure S19 XPS survey spectra of NiCoBP-Br before (red) and after (blue) cycling.

Table S1. Summary of electrochemical performance for as-prepared MOF samples.

Electrodes	Detection limit (μM)	Linear range (mM)	Sensitivity (μA mM^{-1} cm^{-2})
NiCoBP	0.104	0.0005–7.07	1123.28
NiCoBP-Br	0.0665	0.0005- 6.07	1755.51
NiCoBP-I	0.072	0.0005- 6.07	1621.97

Table S2. Comparison of electrochemical performance of recent non-enzymatic glucose sensing with MOF based materials.

Electrodes	Detection limit (µM)	Linear range (mM)	Sensitivity (µA mM^{-1} cm^{-2})	References
Hierarchical sheet-like Ni-BDC/GCE	6.68	0.01–0.8	636	[1]
Co-MOF	0.25	0.0005-8.06	219.67	[2]
Co-MOF/NF	0.0013	0.001-3	10886	[3]
NiCo-MOFNs	0.29	0.001–8	-	[4]
Co$_3$(BTC)$_2$/rGO/GCE	0.33	0.001-0.33	1709	[5]
Nick-cobalt phosphate	0.4	0.002-4.47	302.99	[6]
NiCo-MOFNs	0.29	0.001-8	684.4	[7]
Cu@HHNs	1.97	0.005-3	1594.2	[8]
NiCoBP-Br	0.0665	0.0005- 6.07	1755.5144	This work

References

1. G. Gumilar, Y. V. Kaneti, J. Henzie, S. Chatterjee, J. Na, B. Yuliarto, N. Nugraha, A. Patah, A. Bhaumik and Y. Yamauchi, General synthesis of hierarchical sheet/plate-like M-BDC (M = Cu, Mn, Ni, and Zr) metal-organic frameworks for electrochemical non-enzymatic glucose sensing, *Chem. Sci.*, 2020, **11**, 3644-3655.

2. Q. Li, Z. F. Shao, T. Han, M. B. Zheng and H. Pang, A High-Efficiency Electrocatalyst for Oxidizing Glucose: Ultrathin Nanosheet Co-Based Organic Framework Assemblies, *ACS Sustainable Chem. Eng.*, 2019, **7**, 8986-8992.

3. Y. Li, M. Xie, X. Zhang, Q. Liu, D. Lin, C. Xu, F. Xie and X. Sun, Co-MOF nanosheet array: A high-performance electrochemical sensor for non-enzymatic glucose detection, *Sens. Actuators B Chem.,*2019, **278**, 126-132.

4. W. Li, S. Lv, Y. Wang, L. Zhang and X. Cui, Nanoporous gold induced vertically standing 2D NiCo bimetal-organic framework nanosheets for non-enzymatic glucose biosensing, *Sens. Actuators B Chem.*, 2019, **281**, 652-658.

5. S. Shahrokhian, M. Ezzati and H. Hosseini, Fabrication of a sensitive and fast response electrochemical glucose sensing platform based on co-based metal-organic frameworks obtained from rapid in situ conversion of electrodeposited cobalt hydroxide intermediates,

Talanta, 2020, **210**, 12.

6.   Y. Shu, B. Li, J. Y. Chen, Q. Xu, H. Pang and X. Y. Hu, Facile Synthesis of Ultrathin Nickel-Cobalt Phosphate 2D Nanosheets with Enhanced Electrocatalytic Activity for Glucose Oxidation, *ACS Appl. Mater. Interfaces*, 2018, **10**, 2360-2367.

7.   W. W. Li, S. Lv, Y. Wang, L. Zhang and X. Q. Cui, Nanoporous gold induced vertically standing 2D NiCo bimetal-organic framework nanosheets for non-enzymatic glucose biosensing, *Sens. Actuators B Chem.*, 2019, **281**, 652-658.

8.   Q. Zhu, S. Hu, L. Zhang, Y. Li, C. Carraro, R. Maboudian, W. Wei, A. Liu, Y. Zhang and S. Liu, Reconstructing hydrophobic ZIF-8 crystal into hydrophilic hierarchically-porous nanoflowers as catalyst carrier for nonenzymatic glucose sensing, *Sens. Actuators B Chem.*, 2020, **313**, 128031.